G protein-coupled receptor kinase-5 regulates thrombin-activated signaling in endothelial cells

Chinnaswamy Tiruppathi*†‡, Weihong Yan*†, Raudel Sandoval*, Tabassum Naqvi*, Alexey N. Pronin§, Jeffery L. Benovic§, and Asrar B. Malik*

*Department of Pharmacology, College of Medicine, University of Illinois, Chicago, IL 60612; and §Department of Microbiology and Immunology, Thomas Jefferson University, Philadelphia, PA 19107

Communicated by Ivar Giaever, Rensselaer Polytechnic Institute, Troy, NY, May 8, 2000 (received for review February 14, 2000)

We studied the function of G protein-coupled receptor kinases (GRKs) in the regulation of thrombin-activated signaling in endothelial cells. GRK2, GRK5, and GRK6 isoforms were expressed predominantly in endothelial cells. The function of these isoforms was studied by expressing wild-type and dominant negative (dn) mutants in endothelial cells. We determined the responses to thrombin, which activates intracellular signaling in endothelial cells by cleaving the NH_2 terminus of the G protein-coupled proteinase-activated receptor-1 (PAR-1). We measured changes in phosphoinositide hydrolysis and intracellular Ca^{2+} concentration ($[Ca^{2+}]_i$) in response to thrombin as well as the state of endothelial activation. In the latter studies, the transendothelial monolayer electrical resistance, a measure of the loss of endothelial barrier function, was measured in real time. Of the three isoforms, GRK5 overexpression was selective in markedly reducing the thrombin-activated phosphoinositide hydrolysis and increased $[Ca^{2+}]_i$. GRK5 overexpression also inhibited the thrombin-induced decrease in endothelial monolayer resistance by 75%. These effects of GRK5 overexpression occurred in association with the specific increase in the thrombin-induced phosphorylation of PAR-1. In contrast to the effects of GRK5 overexpression, the expression of the dn-GRK5 mutant produced a long-lived increase in $[Ca^{2+}]_i$ in response to thrombin, whereas dn-GRK2 had no effect. These results indicate the crucial role of the GRK5 isoform in the mechanism of thrombin-induced desensitization of PAR-1 in endothelial cells.

Thrombin activates proteinase-activated receptor-1 (PAR-1) by cleaving the receptor's NH_2-terminal exodomain between Arg-41 and Ser-42 (1), and the newly formed amino terminus binds to the receptor's extracellular domain, thereby activating PAR-1 signaling (1, 2). PAR-1 has been shown to couple functionally to both pertussis toxin-sensitive and -insensitive heterotrimeric G proteins, G_i and G_q (3, 4). We have shown that thrombin by the activation of PAR-1 induces the endothelial cell retraction response (a characteristic feature of the loss of endothelial barrier function) (5–7). PAR-1 activation elicits this response by coupling with the G_q/phospholipase C system (3, 4). We also have shown that thrombin activates mitogen-activated protein kinase to induce PAR-1 expression in endothelial cells, a response chiefly dependent on the binding of PAR-1 to G_i (8).

Although it is clear that thrombin activates PAR-1, which in turn mediates the loss of endothelial barrier function (5–7), the mechanisms responsible for inactivating PAR-1 signaling remain unclear. PAR-1 desensitization after cleavage of the receptor may involve endocytosis and subsequent lysosomal degradation of PAR-1 (9). In addition, G protein-coupled receptor kinases (GRKs) appear to play a key role in inactivating PAR-1, itself a G protein-coupled receptor (GPCR) (10, 11). GRKs are serine/threonine kinases that induce receptor desensitization by the phosphorylation of agonist-occupied or -activated receptors (12, 13). Seven GRK isoforms differing in their posttranslational modification, regulation by phospholipids, and association with G protein subunits (13–18) have been identified. GRK1, GRK4, and GRK7 have limited tissue distribution (13–18). Expression of GRK1 and GRK7 is specific to the retina and expression of GRK4 is limited to the testis (13–18). In contrast, GRK2, GRK3, GRK5, and GRK6 isoforms are widely distributed in multiple cell types (13–18).

In the present study, we specifically analyzed the role of GRK isoforms in the mechanism of desensitization of PAR-1 in endothelial cells. Phosphorylation by GRKs of serine/threonine sites in the COOH terminus of PAR-1 has been linked to the mechanism of desensitization of PAR-1 (1). Coexpression of GRK3 (but not GRK2) with PAR-1 in *Xenopus* oocytes was shown to inhibit thrombin-activated Ca^{2+} signaling (10). Although GRKs can regulate the activity of PAR-1, it is not known which GRKs are expressed in the endothelial cells and which are involved in mediating the desensitization of PAR-1. Thus, we first identified the specific expression of the GRK2, GRK5, and GRK6 isoforms in endothelial cells. We then overexpressed these isoforms in endothelial cells to study their role in the mechanism of inactivation of thrombin-activated signaling. GRK5 overexpression was selective in inhibiting thrombin-activated signaling and further, expression of dominant negative (dn)-GRK5 mutant was selective in prolonging thrombin-activated Ca^{2+} signaling in endothelial cells. These results suggest the crucial role of GRK5 in the mechanism of inactivation of PAR-1 signaling in endothelial cells.

Materials and Methods

Materials. Human α-thrombin was obtained from Enzyme Research Laboratories (South Bend, IN). FBS was from HyClone. PAR-1 antibody (anti-PAR-1 peptide Ab) was raised in rabbits and purified as described (19). dn-GRK2 (K220R) (20) and dn-GRK5 (K215R) in pcDNA3 expression vector, recombinant GRKs (GRK2, GRK5, and GRK6), mAb produced against GRK2 (3A10), and polyclonal Ab raised against the C terminus of GRK5 were prepared as described (16, 20–24). GRK3- and GRK6-specific polyclonal Abs were obtained from Santa Cruz Biotechnology. Fura 2-AM was from Molecular Probes, and electrodes for endothelial monolayer resistance measurements were purchased from Applied Biophysics (Troy, NY).

Abbreviations: GRK, G protein-coupled receptor kinase; PAR-1, proteinase-activated receptor-1; HMEC, human dermal microvascular endothelial cells; dn, dominant negative; $[Ca^{2+}]_i$, intracellular Ca^{2+} concentration; GPCR, G protein-coupled receptor; RT, reverse transcription.

†C.T. and W.Y. contributed equally to this work.

‡To whom reprint requests should be addressed at: Department of Pharmacology (M/C 868), University of Illinois, 835 South Wolcott Avenue, Chicago, IL 60612-7343. E-mail: tiruc@uic.edu.

The publication costs of this article were defrayed in part by page charge payment. This article must therefore be hereby marked "*advertisement*" in accordance with 18 U.S.C. §1734 solely to indicate this fact.

Cell Cultures. Human dermal microvascular endothelial cells (HMEC) (obtained from Edwin W. Ades, Centers for Disease Control and Prevention, Atlanta) were grown to confluence in endothelial basal medium MCDB131 (GIBCO/BRL) supplemented with 10% FBS, 10 ng/ml epidermal growth factor, 2 mM L-glutamine, and 1 μg/ml hydrocortisone. PA317 cell line (ATCC CRL 9078) (25) was grown in DMEM supplemented with 10% FBS. Human pulmonary artery endothelial cells (HPAECs) obtained from Clonetics (San Diego) were grown in EBM-2 medium (Clonetics) supplemented with 10% FBS. Human umbilical vein endothelial cells (HUVECs) obtained from Vec Technologies (Rensselaer, NY) were grown in RPMI 1640 medium supplemented with 10% FBS, 90 μg/ml heparin, 2 mM L-glutamine, and 30 μg/ml endothelial cell growth factor. Primary culture HPAECs and HUVECs passaged between 2 and 4 were used for experiments. Ramos cell line [Burkitt's lymphoma cell line (ATCC CRL-1596)], a human cell line expressing GRK3 (unpublished observation from Santa Cruz Biotechnology) was grown in RPMI 1640 medium containing 10 mM Hepes, pH 7.4, supplemented with 10% FBS and 2 mM L-glutamine in suspension.

GRK Plasmid Construction and Stable Expression in HMEC. Bovine GRK2 cDNA in pBC vector was provided by R. Lefkowitz (Duke University, Durham, NC). pBluescript plasmids containing human cDNA for GRK5 and GRK6 were prepared as described (14, 16). *Hin*dIII fragment of GRK2 cDNA released from pBC-GRK2 was subcloned into retroviral vector pLNCX. *Eco*RI fragments of pBluescript-GRK5 and pBluescript-GRK6 were blunt-ended, connected to *Hin*dIII–*Not*I adaptor (Stratagene), and ligated into *Hin*dIII site in pLNCX. The pLNCXs with sense orientation of GRK2, GRK5, and GRK6 constructs were used for transfecting the packaging cells (PA317) by using Lipofectamine (8). The PA317 cells were screened with 600 μg/ml G418 for 10 days, and surviving cells were grown to confluence (25, 26). PA317-conditioned medium containing retroviral particles was used to infect HMEC as described (25, 26). Four days after infection, cells were trypsinized and seeded in 96-well plates and allowed to grow for 24 h. The cells then were screened with 500 μg/ml G418 for 10 days (26), and the surviving cells were expanded and used for experiments.

Expression of GRK Mutants. dn-GRK2 and dn-GRK5 were transiently expressed in HMEC by using Lipofectamine (8). We determined the transfection efficiency by using green fluorescent protein plasmid. Approximately <50% of HMEC appeared green 48 h after transfection (8).

Reverse Transcription (RT) and PCR. Total RNA was isolated from cells by using Trizol Reagent (GIBCO/BRL) and treated with DNase. Total RNA (3 μg) was reverse-transcribed by using a SuperScript Preamplification kit (GIBCO/BRL). Human GRK3 was amplified by using the following primers: position 1563 forward 5′-AACGGAAACAGTTTATGAAG-3′, position 1995 reverse 5′-GAGGAACTTCGGGGCACGAC-3′, amplifying 433 bp. RT product (2 μl) was amplified in a 50 μl volume containing 1 μM primers and 2 units of *Taq* polymerase. Reaction conditions were 94°C for 30 sec, 45°C for 30 sec, 72°C for 3 min for 35 cycles, and then 72°C for 10 min. PCR products were separated by using 1.7% agarose gel and identified by ethidium bromide staining.

Immunoblot Blot Analysis. HMEC transduced with either pLNCX (mock) or GRK isoforms (GRKs) grown to confluency were washed twice with PBS, pH 7.4 containing 0.1 mM PMSF, 1 μg/ml leupeptin, 1 μg/ml aprotinin, and 1 μg/ml pepstatin. After washing, the cells were scraped and centrifuged at 3,000 $\times$ *g* for 10 min. The cell pellet protein (100 μg) was separated on SDS/PAGE and transferred to a nitrocellulose membrane. The membrane was blocked with 5% nonfat dry milk in Tris-buffered saline with 0.05% Tween-20 (TBST) overnight at 22°C. After washing three times with TBST, the membrane was incubated with respective GRK isoform Abs in TBST with 5% nonfat dry milk for 4 h at 22°C. The membrane then was washed three times with TBST and incubated with either goat anti-mouse IgG or goat anti-rabbit IgG conjugated with peroxidase for 1 h at 22°C. The protein bands were identified by using the ECL method (Pierce).

Phosphoinositide Hydrolysis. Cells were grown in 12-well culture dishes to 70–80% confluence. Cells were washed twice with inositol-free DMEM containing 5% FBS and then cells were incubated with *myo*-[^{3}H]inositol (10 μCi/ml) in inositol-free DMEM containing 5% FBS for 18 h. After labeling, the cells were washed twice with inositol and serum-free DMEM and incubated with 5 mM LiCl for 10 min. The cells then were stimulated with 10 nM thrombin for 1 h at 37°C. The total inositol phosphate formed was extracted and separated on Dowex AG1-X8 formate columns as described (27).

Cytosolic Ca^{2+} Measurement. The cytosolic intracellular Ca^{2+} concentration ($[Ca^{2+}]_i$) in single endothelial cells was measured by fura-2 fluorescence imaging (28). Cells grown on 25-mm diameter glass coverslips were washed twice in Hanks' balanced salt solution (HBSS) and loaded with 3 μM fura-2/AM for 1 h at 25°C. Cells then were washed twice in HBSS and imaged by using an Attofluor RatioVision digital fluorescence microscopy system (Atto Instruments, Rockville, MD) equipped with a Zeiss Axiovert S100 inverted microscope and a F-Fluar $\times$40, 1.3 numerical aperature oil immersion objective. Regions of interest on individual cells were marked and excited at 334 and 380 nm with emission at 520 nm. The increases in 334/380 excitation ratio as a function of $[Ca^{2+}]_i$ was captured at 5-sec intervals. At the end of each experiment, 5 μM ionomycin was added to obtain fluorescence of Ca^{2+}-saturated fura-2 (high $[Ca^{2+}]_i$), and 10 mM EGTA to obtain fluorescence of free fura-2 (low $[Ca^{2+}]_i$). The $[Ca^{2+}]_i$ was calculated based on a K_d of 225 nM with a two-point fit curve.

Transendothelial Electrical Resistance Measurement. Thrombin-induced endothelial cell retraction was measured by the method described by us (29). Endothelial cells were grown to confluence on gelatin-coated gold electrode (5.0×10^{-4} cm^2). The small electrode and the larger counter electrode were connected to a phase-sensitive lock-in amplifier. A constant current of 1 μA was supplied by a 1-V, 4000-Hz AC signal connected serially to 1 MΩ resistor between the small electrode and the larger counter electrode. The voltage between small electrode and large counter electrode was monitored by a lock-in amplifier, stored, and processed by a personal computer. The same computer controlled the output of the amplifier and switched the measurement to different electrodes in the course of an experiment. Before the experiment, cells were incubated in DMEM with 20 mM Hepes, pH 7.4 for 2 h and then thrombin-induced change in endothelial monolayer electrical resistance was measured (7, 29).

PAR-1 Phosphorylation and Immunoprecipitation. Cells grown to confluency in 35-mm dishes were incubated with phosphate-free DMEM for 2 h at 37°C and then incubated with [^{32}P]orthophosphate (100 μCi/dish) for 4 h. After exposure to thrombin for different time intervals, cells were washed once with ice-cold PBS containing 1 μM okadaic acid and 1 mM sodium orthovanadate (wash buffer), twice with wash buffer containing 2 mg/ml albumin, and another time with wash buffer alone. Cells were lysed with lysis buffer (50 mM Tris/150 mM NaCl/1 mM EDTA/0.5% sodium deoxycholate/1% NP-40/0.1% SDS/1 mM sodium orthovanadate/1 μg/ml leupeptin/1 μg/ml pepstatin A/1 μg/ml aproptinin/1 mM PMSF/1 μM okadaic acid/50 nM calyculin A) at 4°C for 30 min. The lysate was centrifugated at 13,000 $\times$ *g* for 10 min and supernatant containing equal amount of protein was precleared by

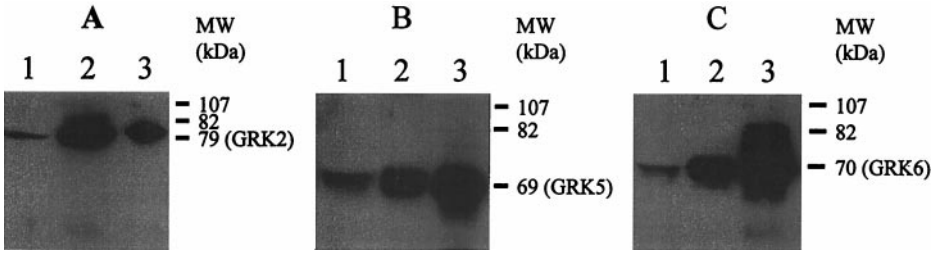

Fig. 1. Determination of GRK isoform expression in endothelial cells by immunoblotting. Total cell protein (100 μg/lane) was subjected to SDS/PAGE and blotted with GRK-specific antibodies. Other details are described in *Materials and Methods*. (*A*) Expression of GRK2. Lane 1, HMEC-mock; lane 2, HMEC-GRK2; lane 3, RC-GRK2 (12.5 ng). (*B*) Expression of GRK5. Lane 1, HMEC-mock; lane 2, HMEC-GRK5; lane 3, RC-GRK5 (25 ng). (*C*) Expression of GRK6. Lane 1, HMEC-mock; lane 2, HMEC-GRK6; lane 3, RC-GRK6 (25 ng). Results are representative of four experiments in each group.

preimmune IgG and protein A-Sepharose beads for 1 h at 4°C. The supernatant was collected by centrifugation and incubated with anti-PAR-1 peptide Ab overnight at 4°C. The incubation was continued for another hour after adding protein A-Sepharose beads. The beads were pelleted, washed four times with wash buffer, and subjected to SDS/PAGE. The gels were dried and exposed to Kodak film for 24 h. Autoradiograms were scanned and the PAR-1 phosphorylation was quantitated by National Institutes of Health IMAGE version 1.6.

Statistics. Statistical analysis was performed by using the two-tailed Student's *t* test.

Results

Selective Expression of GRK2, GRK5, and GRK6 Isoforms in Endothelial Cells. We determined the expression GRK isoforms in endothelial cells by immunoblotting (details in *Materials and Methods*). GRK proteins were identified by using the recombinant GRK proteins. GRK2, GRK5, and GRK6 proteins from endothelial cells comigrated with the respective recombinant proteins (Fig. 1), indicating that GRK2, GRK5, and GRK6 isoforms were constitutively expressed in HMEC. We also determined the expression of GRK isoforms in human umbilical vein endothelial cells and human pulmonary artery endothelial cells; these cells showed the pattern of expression of GRK isoforms similar to the HMEC (data not shown). To address the presence of GRK3 in HMEC, we used the GRK3-positive Ramos cell line in which there was clear evidence of GRK3 mRNA as well as protein expression (Fig. 2). Using RT-PCR and immunoblotting, we were not able to detect the expression of GRK3 (≈70-kDa protein) in HMEC (Fig. 2). We also could not detect GRK3 in other endothelial cell types (data not shown). The present findings indicate that GRK3 is not constitutively present in HMEC or the other endothelial cells studied.

We overexpressed endothelial cell-specific GRK isoforms to study their function in the regulation of thrombin-activated responses in endothelial cells. To induce GRK2 expression, we transduced bovine GRK2 cDNA in HMEC. In vector-transduced cells (mock), level of GRK2 (79-kDa protein) expression did not change from control HMEC; therefore, we used vector transduced cells as control (Fig. 1*A*, lane 1). In cells transduced with pLNCX-GRK2, GRK2 expression increased 4- to 6-fold (Fig. 1*A*, lane 2). To overexpress GRK5 and GRK6, we used human cDNA constructs. Fig. 1*B* shows GRK5 (≈69 kDa) isoform expression. Transduction with GRK5 resulted in significantly increased expression of GRK5 (Fig. 1*B*, lane 2). Fig. 1*C* shows the expression of GRK6 (≈70-kDa protein). GRK6 expression was increased 3- to 4-fold in GRK6-transduced cells (Fig. 1*C*, lane 2). We also determined the mRNA expression in GRK2, GRK5, and GRK6 overexpressing cells by RT-PCR. The mRNA expression levels were increased 2- to 4-fold in these cells compared with control (data not shown).

GRK5 Overexpression Inhibits Thrombin-Induced Phosphoinositide Hydrolysis and Ca^{2+} Signaling. We measured thrombin-induced phosphoinositide hydrolysis in HMEC, mock, and cells overexpressing GRK2, GRK5, and GRK6 isoforms. Thrombin-induced phosphoinositide hydrolysis was suppressed by ≈70% in the GRK5-overexpressing cells compared with HMEC and mock, whereas thrombin-induced phosphoinositide hydrolysis was not significantly affected in cells expressing the GRK2 or GRK6 isoform (Fig. 3). Thus, these results indicate that GRK5 specifically inhibits thrombin-activated phosphoinositide hydrolysis in endothelial cells.

We measured thrombin-induced increases in $[Ca^{2+}]_i$ to study whether inhibition of phosphoinositide hydrolysis was coupled to

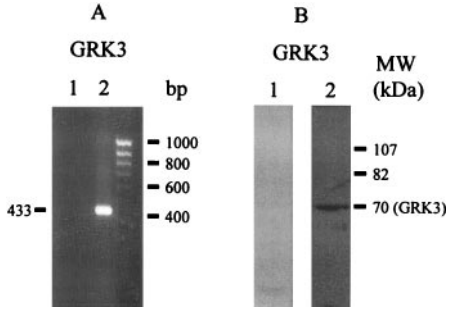

Fig. 2. Absence of GRK3 expression in HMEC. Experimental conditions are described in Fig. 1 legend and in *Materials and Methods*. (*A*) RT-PCR. Lane 1, HMEC; lane 2, Ramos cell line (GRK3-positive); RT samples were PCR-amplified with human GRK3 primers. (*B*) Immunoblotting. Lane 1, HMEC; lane 2, Ramos. GRK3-specific Ab was used for immunoblotting. Results are representative of four experiments in each group.

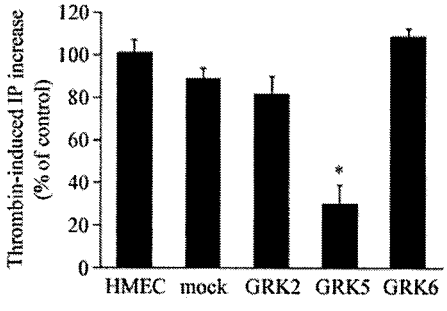

Fig. 3. Effects of GRK isoform overexpression on thrombin-induced phosphoinositide hydrolysis. Experimental conditions are described in *Materials and Methods*. Cells were stimulated with 10 nM thrombin for 1 h and total inositol phosphates formed were measured. Results are mean ± SE of three separate experiments carried out in triplicate. * indicates difference from HMEC ($P < 0.001$).

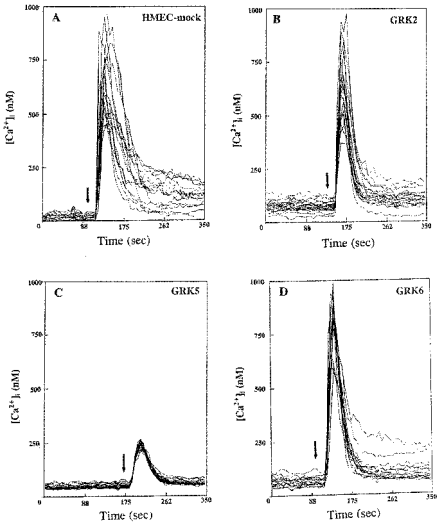

Fig. 4. Effects of GRK overexpression on thrombin-induced increase in $[Ca^{2+}]_i$. The changes in $[Ca^{2+}]_i$ in single cells were measured in response to 10 nM thrombin. In each experiment, 20–50 cells were selected to measure change in $[Ca^{2+}]_i$. The position of arrow indicates the time the cells were stimulated with thrombin. Other details are described in *Materials and Methods*. The experiment was repeated three times. Results from a representative experiment are shown. (*A*) HMEC-mock. (*B*) HMEC-GRK2. (*C*) HMEC-GRK5. (*D*) HMEC-GRK6. Table 1 summarizes the results from three experiments.

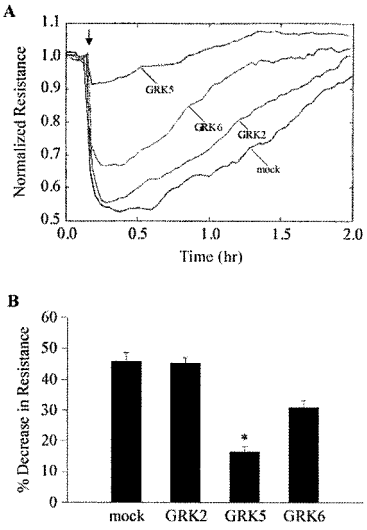

Fig. 5. Effect of GRK isoform overexpression on change in thrombin-induced transendothelial monolayer electrical resistance. (*A*) HMEC-mock and HMEC-transduced with different GRK isoforms were incubated in serum-free medium for 2 h and then the thrombin (10 nM)-induced resistance change was measured. Arrow represents the time point of thrombin addition. (*B*) Bar graph shows thrombin-induced decrease in electrical resistance. $n = 23$ for HMEC-mock; $n = 8$ for HMEC-GRK2; $n = 13$ for HMEC-GRK5; $n = 17$ for HMEC-GRK6. Bars indicate ± SEM; * indicates $P < 0.01$ from other groups.

failure of the GRK5-expressing cells to mobilize intracellular Ca^{2+}. In control cells (mock), thrombin (10 nM) caused an increase in $[Ca^{2+}]_i$ with a peak value of 675 ± 55 nM (Fig. 4*A* and Table 1). Basal $[Ca^{2+}]_i$ values in all groups were similar (Table 1). In GRK2-and GRK6-overexpressing cells, the thrombin-induced increases in $[Ca^{2+}]_i$ were similar to mock (Fig. 4 *B* and *D* and Table 1). However, in GRK5-overexpressing cells, thrombin-induced increase in $[Ca^{2+}]_i$ was reduced by 3-fold compared with control (Fig. 4*C* and Table 1). We also determined the effects of PAR-1 activating peptide (TRAP) on Ca^{2+} signaling in these cells. TRAP-induced increase in $[Ca^{2+}]_i$ in the GRK2- or GRK6-overexpressing cells was similar to control, whereas the response was significantly reduced in the GRK5-overexpressing cells (data not shown).

Effects of Overexpression of GRK Isoforms on Thrombin-Induced Endothelial Cell Retraction. To determine the functional consequences of GRK isoform expression, we studied the thrombin-induced endothelial cell retraction response [i.e., a measure of cell shape change and increased transendothelial permeability (29)], a response mediated by PAR-1 activation (7). In control cells, thrombin caused ≈40% decrease in electrical resistance (Fig. 5). GRK2 overexpression did not alter this response (Fig. 5), whereas GRK5 overexpression inhibited the thrombin-induced decrease in monolayer resistance by ≈75% (Fig. 5). In GRK6-overexpressing cells, inhibition was significantly less (≈20%) compared with control (Fig. 5).

Table 1. GRK5 overexpression selectively prevents thrombin-induced increase in $[Ca^{2+}]_i$

Cell type	Basal $[Ca^{2+}]_i$, nM	Peak $[Ca^{2+}]_i$, nM	*n*
HMEC-mock	35 ± 3	675 ± 55	56
GRK2	53 ± 4	690 ± 35	60
GRK5	42 ± 3	224 ± 15*	60
GRK6	46 ± 4	720 ± 35	50

Values are shown as means ± SEM. *n* = number of cells in each group.
*Significance from other groups; $P < 0.001$.

GRK5 Overexpression Increases Phosphorylation of PAR-1. We determined the effects of GRK overexpression on PAR-1 phosphorylation. As immunoprecipitations were carried out to assess phosphorylation of PAR-1, we first tested the specificity of anti-PAR-1 peptide Ab by using endothelial cell lysates. The anti-PAR-1 peptide Ab reacted with a major 60-kDa protein (Fig. 6*A*) from the endothelial cell lysate. Inclusion of the antigenic PAR-1 peptide during immunoblotting prevented the reactivity of anti-PAR-1 peptide Ab with 60-kDa protein, indicating that the anti-PAR-1 peptide Ab reacted specifically with PAR-1 (Fig. 6*A*). We metabolically labeled cells with [^{32}P]orthophosphate and stimulated with thrombin for different time intervals. Cells were lysed and PAR-1 was immunoprecipitated (see details in *Materials and Methods*). Basal PAR-1 phosphorylation was low in untreated control cells. After thrombin challenge, PAR-1 phosphorylation increased significantly and reached maximum level in 15 sec; this level was maintained for at least 30 sec (Fig. 6 *B* and *C*). In GRK2-expressing cells, basal phosphorylation was increased ≈2-fold, but the thrombin-induced PAR-1 phosphorylation was similar to control (Fig. 6 *B* and *C*). In GRK5-expressing cells, basal phosphorylation of PAR-1 increased 3-fold and thrombin caused even a further increase in PAR-1 phosphorylation (Fig. 6 *B* and *C*). In contrast, in GRK6-expressing cells, basal phosphorylation of PAR-1 was increased and thrombin treatment did not further increase the phosphorylation (Fig. 6 *B* and *C*).

dn-GRK5 Expression Augments Thrombin-Induced Increase in $[Ca^{2+}]_i$. To address the role of endogenous GRK isoforms, we transiently expressed the dn-GRK2 and dn-GRK5 in HMEC and measured thrombin-induced increase in $[Ca^{2+}]_i$. Expression of pcDNA3 vector or dn-GRK2 did not affect thrombin-induced increase in $[Ca^{2+}]_i$ compared with control cells (Fig. 7 *A* and *B*). However, expression of dn-GRK5 produced a prolonged increase in $[Ca^{2+}]_i$ in about 50% of cell population (Fig. 7*C*). In vector or dn-GRK2 expressing cells, thrombin produced a transient in-

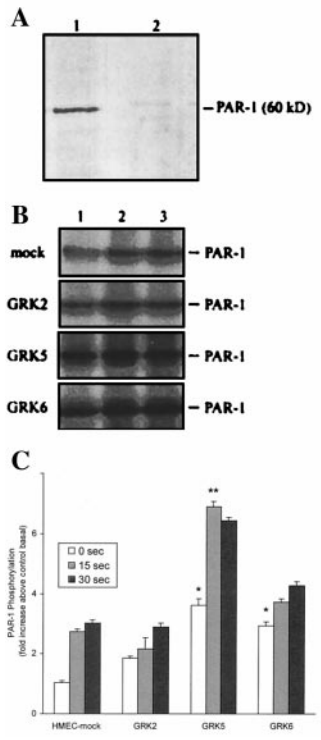

Fig. 6. (*A*) Immmunoblotting of HMEC lysate with anti-PAR-1 peptide Ab. HMEC lysate (100 μg of protein) was separated on SDS/PAGE and transferred to nitrocellulose membrane strips. Strips were incubated with anti-PAR-1 peptide Ab (10 μg/ml) in the presence and absence of PAR-1 antigenic peptide (20 μg/ml). Other details are described in *Materials and Methods*. Lane 1, control; lane 2, incubated with PAR-1 peptide TR 70–99. (*B*) Effects of GRK overexpression on phosphorylation of PAR-1. HMEC transduced with vector or vector in combination with GRK isoforms were labeled with ^{32}P-orthophosphate and exposed to thrombin (10 nM) for 0 sec, 15 sec, and 30 sec. Cells were washed, lysed, and immunoprecipitated, and proteins were resolved by SDS/PAGE. Other details are described in *Materials and Methods*. Representative autoradiogram is shown in *B*. Lane 1, cells exposed to thrombin for 0 sec; lanes 2 and 3, cells exposed to thrombin for 15 and 30 sec, respectively. (*C*) ^{32}P-labeling was quantified and expressed as fold increase over the control (HMEC-mock) basal value. Values are shown as mean ± SEM from 4–6 experiments in each group. * = $P < 0.01$; ** = $P < 0.005$.

crease in $[Ca^{2+}]_i$ and the level returned to baseline values within 3–4 min. In dn-GRK5 expressing cells, thrombin produced a long-lived increase in $[Ca^{2+}]_i$ (Fig. 7*C*) (up to 30 min).

Discussion

The phosphorylation of activated GPCRs by GRKs is a primary mechanism mediating the desensitization of receptors (12, 13). In the present study, we examined the role of GRKs expressed in endothelial cells in mediating PAR-1 desensitization. We observed that GRK2, GRK5, and GRK6 were selectively expressed in endothelial cells. Although the GRK3 isoform is expressed in many tissues (16–24), it was not detectable in cultured endothelial cells.

As an approach to addressing the effects of the endothelial cell GRK isoforms in regulating thrombin-activated signaling, we used the retroviral method to stably overexpress these GRK isoforms in HMEC (25, 26). We determined whether their overexpression in endothelial cells affected the phosphorylation of PAR-1, the GPCR that upon cleavage by thrombin activates intracellular Ca^{2+} signaling and induces the loss of endothelial barrier function (5–7). We showed that overexpression of GRK2 in HMEC had no effect on either thrombin-activated signaling or phosphorylation of PAR-1. These results are consistent with the finding that GRK2 expression in *Xenopus* oocytes does not prevent Ca^{2+} signaling activated by the simultaneous coexpression of PAR-1 (10). We also showed that GRK6 overexpression in HMEC did not significantly alter thrombin-induced phosphoinositide hydrolysis and the increase in $[Ca^{2+}]_i$ as well as PAR-1 phosphorylation. In contrast, GRK5 overexpression markedly interfered with thrombin-induced phosphoinositide hydrolysis and increase in $[Ca^{2+}]_i$, and induced the phosphorylation of PAR-1. In other studies, we showed that inhibiting the function of endogenous GRK5 by expressing dn-GRK5 mutant in HMEC produced a prolonged increase in $[Ca^{2+}]_i$ in response to thrombin. As evidence that GRK5 regulates PAR-1 activated endothelial responses, we showed that GRK5 overexpression inhibited ≈75% of the thrombin-induced decrease in endothelial cell resistance. This finding suggests the important role of GRK5 in modulating the endothelial barrier function.

Studies have shown that thrombin activation of PAR-1 in Rat1 cells and human embryonic kidney 293 cells stably transfected with the receptor induced the phosphorylation of PAR-1 within minutes (9, 30). In the present study, we showed that PAR-1 in endothelial cells was phosphorylated within 15 sec after activation by thrombin. This rapid phosphorylation of PAR-1 is consistent with the time course reported for GRK-induced receptor desensitization (31), but it is considerably shorter than the 30 min required for heterologous desensitization of receptors induced by protein kinase C activation (32). Moreover, these results suggest that GRK5 is specific in mechanism of phosphorylation because the thrombin challenge of the GRK5-expressing endothelial cells selectively augmented PAR-1 phosphorylation.

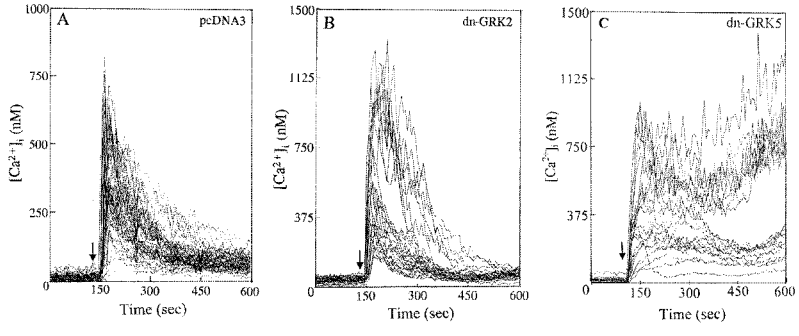

Fig. 7. Effects of dn-GRK2 and dn-GRK5 expression on thrombin-induced Ca^{2+} signaling in endothelial cells. dn-GRK2 and dn-GRK5 were transiently expressed in HMEC by using Lipofectamine (8). HMEC, grown on gelatin-coated glass coverslips to 50–70% confluency, were transfected with 500 ng of plasmid DNA (pcDNA3, dn-GRK2, or dn-GRK5). Other details are described in *Materials and Methods*. Cells were allowed to grow for 72 h and then were used for intracellular Ca^{2+} measurement. The experiment was repeated four times. (*A*) pcDNA3 (vector) transfected. (*B*) dn-GRK2 transfected. (*C*) dn-GRK5 transfected.

This conclusion is distinct from a report (10) showing that coexpression of GRK3 with PAR-1 in *Xenopus* oocytes inhibited thrombin-activated Ca^{2+} signaling. Although GRK3 expression can regulate PAR-1 function in the *Xenopus* oocyte and possibly other cell types, this isoform is unlikely to be important in modulating PAR-1 activity in endothelial cells because it is not significantly expressed in these cells.

We observed a high level of basal phosphorylation of PAR-1 in the GRK2-, GRK5-, and GRK6-overexpressing endothelial cells. Increased basal phosphorylation of GPCRs also has been reported in other GRK transfection studies in intact cells (33, 34). The increase in basal receptor phosphorylation may be the result of increased membrane association of the expressed GRKs with the GPCRs (13).

Thrombin mediates increased endothelial permeability by causing endothelial cell retraction, resulting in the formation of interendothelial gaps (35). Thrombin-induced endothelial cell retraction is associated with increased $[Ca^{2+}]_i$ and Ca^{2+}-dependent phosphorylation of actin-associated cytoskeletal proteins (35). We have shown that PAR-1 activation causes endothelial cell retraction, resulting in increased endothelial permeability to macromolecules (6–8). In the present study, we addressed the effects of expression of GRK isoforms in the mechanism of thrombin-induced endothelial cell shape change (i.e., cell retraction) by measuring kinetics in real time of the decrease in endothelial monolayer resistance. GRK2 and GRK6 overexpression in HMEC did not significantly alter thrombin-induced decrease in transendothelial electrical resistance. In contrast, GRK5 overexpression inhibited ≈75% of thrombin-induced decrease in endothelial cell resistance. These results support an important role of GRK5 in functionally inactivating PAR-1 signaling in endothelial cells, and thereby preventing thrombin-induced endothelial cell retraction response.

Dysregulation of GRKs may be important in pathological processes associated with inappropriate GPCR activation responses. Lymphocytes from hypertensive subjects showed increased GRK activity and increased expression of GRK2 (36), suggesting that increased GRK activity may underlie the reduction in β-adrenergic responsiveness in hypertension. Increased GRK activity and GRK expression also may be associated with the development of heart failure (37). Cardiac-specific overexpression of GRK5 in transgenic mice augmented the desensitization of β-adrenergic receptors, whereas it had no effect on the activity of angiotensin II receptors (38). In a similar vein, our study indicates that overexpression of GRK5 in endothelial cells prevented the increase in endothelial permeability in response to thrombin. Thus, the results suggest a potentially important role of GRK5 in regulating vascular endothelial permeability in inflammatory states.

Expression of GRK2 and GRK6 significantly increased the basal phosphorylation of PAR-1, but it did not alter thrombin-activated phosphoinositide hydrolysis and increase in $[Ca^{2+}]_i$. A possible explanation of this finding is that the arrestin proteins associated with receptor internalization may not have been activated after phosphorylation induced by GRK2 and GRK6 (39). Another explanation for the lack of effect of GRK2 and GRK6 overexpression may be the requirement of phosphorylation specific sites in the cytoplasmic domains of PAR-1 needed to induce receptor desensitization (1, 13).

The COOH terminus of PAR-1 contains the consensus serine/threonine phosphorylation sites for GRKs (1). Expression in the Rat1 cell line of the carboxyl tail-truncated PAR-1 or the PAR-1 mutant in which serine and threonine residues in the carboxyl tail are converted to alanine produced persistent signaling in response to thrombin (40, 41). These mutant receptors also failed to internalize upon activation with thrombin (40, 41). In the present study, we showed that the overexpression of GRK5 inhibited the thrombin-activated phosphoinositide hydrolysis and Ca^{2+} signaling and prevented thrombin-induced decrease in endothelial monolayer resistance. Moreover, the expression of dn-GRK5 (but not dn-GRK2) prolonged the Ca^{2+} signaling in response to thrombin, an observation consistent with the augmented Ca^{2+} signaling observed with carboxyl tail-truncated or mutated PAR-1 constructs (40, 41).

In summary, we studied the effects of endothelial cell-specific GRK isoforms, GRK2, GRK5, and GRK6, in regulating the desensitization of PAR-1. Overexpression of GRK2 and GRK6 isoforms did not significantly alter PAR-1-activated phosphoinositide hydrolysis and Ca^{2+} signaling in endothelial cells. In contrast, overexpression of the GRK5 isoform markedly increased agonist-induced phosphorylation of PAR-1 and inhibited PAR-1-mediated endothelial cell retraction. Inhibition of the function of endogenous GRK5 by expressing dn-GRK5 produced long-lived Ca^{2+} signaling in response to thrombin in endothelial cells. These results indicate a critical role for GRK5 in regulating PAR-1 signaling in endothelial cells.

This work was supported by National Institutes of Health Grants GM58531, HL45638, and GM44944.

1. Vu, T. K. H., Hung, D. T., Wheaton, V. I. & Coughlin, S. R. (1991) *Cell* **64,** 1057–1068.
2. Gerstzen, R. E., Chen, J. I., Ishii, M., Wang, L., Nanevlez, T., Turck, C. W., Vu, T. K. H. & Coughlin, S. R. (1994) *Nature (London)* **368,** 648–651.
3. Grand, J. A. R., Turnell, A. S. & Grabham, P. W. (1996) *Biochem. J.* **313,** 353–368.
4. Dery, O., Corvera, C. U., Steinhoff, M. & Bunnett, N. W. (1998) *Am. J. Physiol.* **274,** C1429–C1452.
5. Garcia, J. G. N., Patterson, C., Bahler, C., Aschner, J., Hart, C. M. & English, D. (1993) *J. Cell. Physiol.* **156,** 541–549.
6. Lum, H., Anderson, T. T., Siflinger-Birnboim, A., Tiruppathi, C., Goligorsky, M. S. & Malik, A. B. (1993) *J. Cell. Biol.* **120,** 1491–1499.
7. Ellis, C. A., Tiruppathi, C., Sandoval, R., Niles, W. D. & Malik, A. B. (1999) *Am. J. Physiol.* **276,** C38–C45.
8. Ellis, C. A., Malik, A. B., Gilchrist, A., Hamm, H., Sandoval, R., Voyno-Yasenetskaya, T. & Tiruppathi, C. (1999) *J. Biol. Chem.* **274,** 13718–13727.
9. Hein, L., Ishii, K., Coughlin, S. R. & Kobilka, B. K. (1994) *J. Biol. Chem.* **269,** 27719–27726.
10. Ishii, K., Chen, J., Ishii, M., Koch, W. J., Freedman, N. J., Lefkowitz, R. J. & Coughlin, S. R. (1994) *J. Biol. Chem.* **269,** 1125–1130.
11. Hoxie, J. A., Ahuja, M., Belmonte, E., Pizarro, S., Parton, R. & Brass, L. F. (1993) *J. Biol. Chem.* **268,** 13756–13763.
12. Palczewski, K. & Benovic, J. L. (1991) *Trends Biochem. Sci.* **16,** 387–391.
13. Premont, R. T., Inglese, J. & Lefkowitz, R. J. (1995) *FASEB J.* **9,** 175–182.
14. Benovic, J. L. & Gomez, J. (1993) *J. Biol. Chem.* **268,** 19521–19527.
15. Benovic, J. L., Deblasi, A., Stone, W. C., Caron, M. G. & Lefkowitz, R. J. (1989) *Science* **246,** 235–240.
16. Kunapuli, P., Onorato, J. J., Hosey, M. M. & Benovic, J. L. (1994) *J. Biol. Chem.* **269,** 1099–1105.
17. Kunapuli, P. & Benovic, J. L. (1993) *Proc. Natl. Acad. Sci. USA* **90,** 5588–5592.
18. Hisatomi, O., Matsuda, S., Satoh, T., Kotaka, S., Imanshi, Y. & Tokunaga, F. (1998) *FEBS Lett.* **424,** 159–164.
19. Yan, W., Tiruppathi, C., Qiao, R., Lum, H. & Malik, A. B. (1996) *J. Cell. Physiol.* **166,** 561–567.
20. Kong, G., Penn, R. & Benovic, J. L. (1994) *J. Biol. Chem.* **269,** 13084–13087.
21. Pronin, A. N. & Benovic, J. L. (1997) *J. Biol. Chem.* **272,** 3806–3812.
22. Loudon, R. P., Perussia, B. & Benovic, J. L. (1996) *Blood* **88,** 4547–4557.
23. Kim, C. M., Dion, S. B., Onorato, J. J. & Benovic, J. L. (1993) *Receptor* **3,** 39–55.
24. Loudon, R. P. & Benovic, J. L. (1994) *J. Biol. Chem.* **269,** 22691–22697.
25. Miller, A. D. & Buttimore, C. (1986) *Mol. Cell. Biol.* **6,** 2895–2902.
26. Nagpala, P. G., Malik, A. B., Vuong, P. T. & Lum, H. (1996) *J. Cell. Physiol.* **166,** 249–255.
27. Freedman, N. J., Ament, A. S., Oppermann, M., Stoffel, R. H., Exum, S. T. & Lefkowitz, R. J. (1997) *J. Biol. Chem.* **272,** 17734–17743.
28. Brandoli, C., Sanna, A., De Bernardi, M. A., Follesa, P., Brooker, G. & Mocchetti, I. (1998) *J. Neurosci.* **18,** 7953–7961.
29. Tiruppathi, C., Malik, A. B., Del Vecchio, P. J., Keese, C. R. & Giaever, I. (1992) *Proc. Natl. Acad. Sci. USA* **89,** 7919–7923.
30. Vouret-Craviari, V., Auberger, P., Pouyssegur, J. & Obberghen-Schilling, E. V. (1995) *J. Biol. Chem.* **270,** 4813–4821.
31. Roth, N. S., Campbell, P. T., Caron, M. G., Lefkowitz, R. J. & Lohse, M. J. (1991) *Proc. Natl. Acad. Sci. USA* **88,** 6201–6204.
32. Yan, W., Tiruppathi, C., Lum, H., Qiao, R. & Malik, A. B. (1998) *Am. J. Physiol.* **274,** C387–C395.
33. Tiberi, M. S., Nash, R., Bertrand, L., Lefkowitz, R. J. & Caron, M. G. (1996) *J. Biol. Chem.* **271,** 3771–3778.
34. Diviani, D., Lattion, A. L., Larbi, N., Kunapuli, P., Pronin, A., Benovic, J. L. & Cotecchia, S. (1996) *J. Biol. Chem.* **271,** 5049–5058.
35. Lum, H. & Malik, A. B. (1994) *Am. J. Physiol.* **267,** L223–L241.
36. Gros, R., Benovic, J. L., Tan, C. M. & Feldman, R. D. (1997) *J. Clin. Invest.* **99,** 2087–2093.
37. Ping, P., Gelzer-Bell, R., Roth, D. A., Kiel, D., Insel, P. A. & Hammond, H. K. (1995) *J. Clin. Invest.* **95,** 1271–1280.
38. Rockman, H. A., Choi, D. J., Rahman, N. U., Akhter, S. A., Lefkowitz, R. J. & Koch, W. J. (1996) *Proc. Natl. Acad. Sci. USA.* **93,** 9954–9959.
39. Ferguson, S. S. G., Barak, L. S., Zhang, J. & Caron, M. G. (1996) *Can. J. Physiol. Pharmacol.* **74,** 1095–1110.
40. Shapiro, M. J., Trejo, J., Zeng, D. & Coughlin, S. R. (1996) *J. Biol. Chem.* **271,** 32874–32880.
41. Sambrano, G. R. & Coughlin, S. R. (1999) *J. Biol. Chem.* **274,** 20178–20184.